J Nanopart Res (2008) 10:1193–1202
DOI 10.1007/s11051-007-9353-0

RESEARCH PAPER

UV-induced synthesis, characterization and formation mechanism of silver nanoparticles in alkalic carboxymethylated chitosan solution

Ling Huang · Maolin L. Zhai · Dewu W. Long · Jing Peng · Ling Xu · Guozhong Z. Wu · Jiuqiang Q. Li · Genshuan S. Wei

Received: 21 October 2007 / Accepted: 24 December 2007 / Published online: 18 January 2008

Abstract The silver nanoparticles (AgNPs) were synthesized in an alkalic aqueous solution of silver nitrate ($AgNO_3$)/carboxymethylated chitosan (CMCTS) with ultraviolet (UV) light irradiation. CMCTS, a water-soluble and biocompatible chitosan derivative, served simultaneously as a reducing agent for silver cation and a stabilizing agent for AgNPs in this method. UV–vis spectra and transmission electron microscopy (TEM) images analyses showed that the pH of $AgNO_3$/CMCTS aqueous solutions, the concentrations of $AgNO_3$ and CMCTS can affect on the size, amount of synthesized AgNPs. Further by polarized optical microscopy it was found that the CMCTS with a high molecular weight leads to a branch-like AgNPs/CMCTS composite morphology. The diameter range of the AgNPs was 2–8 nm and they can be dispersed stably in the alkalic CMCTS solution for more than 6 months. XRD pattern indicated that the AgNPs has cubic crystal structure. The spectra of laser photolysis of $AgNO_3$/CMCTS aqueous solutions identified the early reduction processes of silver cations (Ag^+) by hydrated electron (e^-_{aq}) formed by photoionization of CMCTS. The rate constant of corresponding reduction reaction was $5.0 \times 10^9\ M^{-1}\ s^{-1}$.

Keywords Silver nanoparticle · AgNPs/CMCTS composite · UV light irradiation · Laser photolysis · Surface plasmon band · Colloids

L. Huang · M. L. Zhai (✉) · J. Peng · L. Xu · J. Q. Li · G. S. Wei
Beijing National Laboratory for Molecular Sciences, Department of Applied Chemistry, College of Chemistry and Molecular Engineering, Peking University, Beijing 100871, China
e-mail: mlzhai@pku.edu.cn

D. W. Long · G. Z. Wu
Shanghai Institute of Applied Physics, Chinese Academy of Sciences, Shanghai 201800, China

Introduction

In recent years, nanoscale metal and semiconductor particles have attracted considerable attention due to their unique chemical and physical properties. For example, the catalytic activity, novel electronic, optic and magnetic properties, which are very different with those of the bulk, will appear to show marvellous potential of application in some fields, such as biotechnology (Hayward et al. 2000), information science (Belloni 1996), and material science (Henglein 1998; Sudeep and Kamat 2005). During the past several years, numerous physical or chemical methods have been found to synthesize nanoparticles. However, in some chemical methods, both a reducing agent, such as sodium borohydride ($NaBH_4$) (Van Hyning et al. 2001), hydrazine (Sakai et al. 2006), and *N*,*N*-dimethylformamide (Pastoriza-Santos and Liz-Marzan 2002), and a stabilizing agent were required. For example, various metal nanoparticles

were synthesized, including silver (Ag) (Huang et al. 2004), gold (Au). (Esumi et al. 2003; Huang et al. 2005; Huang et al. 2004), platinum (Pt) (Huang et al. 2004), and palladium (Pd) (Huang et al. 2004) by the reduction of corresponding metal cations with $NaBH_4$ in the presence of chitosan as the stabilizing agent. Because these chemicals which possessing a high reductive ability should be used carefully and probably result in the potential environmental risk, scientists kept looking for other convenient and green synthetic methods and had made some progress. For instance, Raveendran et al. used β-D-glucose as a reducing agent and soluble starch as a capping material to synthesize AgNPs by maintaining the reactive solution at 40 °C for 20 h (Raveendran et al. 2003). Furthermore, some reductive polysaccharides such as dextrin (Cao et al. 2005), cellulose acetate nanofibers (Son et al. 2006), and chitosan (Huang and Yang 2004a, b) were also utilized as both the reducing agent and capping materials in the synthesis of metal nanoparticles, but these synthetic methods have some disadvantages for their special reactive technique or a long reactive time. Some physical methods, such as photo-irradiation (UV, Near-IR), ultrasonic, γ-ray/electron beam irradiation, and high-temperature heating were utilized to synthesize metal nanoparticles, and the size of nanoparticle can be modified by altering the parameters, such as the temperature of solution, the intensity of energy, and the concentration of reagent. For example, Bogle et al. (Bogle et al. 2006) synthesized silver nanoparticles (AgNPs) by irradiating the silver nitrate ($AgNO_3$) and poly-vinyl alcohol solutions with an electron beam. Fang et al. (Fang et al. 2004) synthesized Pd nanoparticles on silicon under UV irradiation.

Chitosan, composed of D-glucosamine units, is a kind of natural cationic macromolecule, which possessed an excellent bioactivity and biocompatibility. It is reported that chitosan could be used as a stabilizer in the preparation of Ag (Huang and Yang 2004b; Huang et al. 2004) and Au (Esumi et al. 2003; Huang et al. 2005; Huang and Yang 2004a) nanoparticles in the chemical reduction method too. Chan and his co-workers (Cheng et al. 2005) reported a novel approach to prepare polypyrrole-chitosan hollow nanospheres containing AgNPs in the core by UV light irradiation, using chitosan as a stabilizer as well as a reducing agent. However, the reaction could only be occurred in the acidic solutions because of the poor solubility of chitosan in the neutral and alkalic solutions. It is known that the solubility of chitosan in the neutral or alkalic solutions can be improved remarkably by introducing the carboxymethyl groups to the chitosan molecules, and the structure of carboxymethylated chitosan (CMCTS) is similar to that of an amino acid because CMCTS has both amino groups and carboxyl groups in the molecules. In our previous work, the effects of γ-ray irradiation, laser photolysis, and pulse radiolysis on CMCTS have been investigated in detail (Huang et al. 2007; Zhai et al. 2004b, c), and we found that CMCTS have a strong reactive activity with some active species such as a hydroxyl radicals (·OH), a hydrogen atom (·H), and a hydrated electron (e^-_{aq}). Further laser flash photolysis experiments on CMCTS in aqueous solutions showed that CMCTS can released the e^-_{aq} with the irradiation of a laser beam (Zhai et al. 2004), which is a potential reducing agent for some metal cations. What's more, because the CMCTS was recognized as a non-toxic, multifunctional, biocompatible and biodegradable biomass resource (Chen et al. 2006), we can concluded that metal nanoparticles dispersed in a CMCTS matrix should have a better biocompatibility than those prepared in the non-green methods.

In this paper, we used CMCTS as both a reducing agent and a stabilizing agent to synthesize AgNPs by the UV light irradiation. Some factors, such as pH, the concentrations of $AgNO_3$, the concentrations and the molecular weight of CMCTS on the morphology of AgNPs and AgNPs/CMCTS composites were all studied. Furthermore, the laser photolysis technique was used to investigate the formation mechanism of AgNPs in the CMCTS aqueous solutions. In this method, cubic crystal AgNPs can be synthesized facilely and dispersed stably in the alkalic CMCTS solution for more than 6 months. The utilization of nontoxic, biocompatible CMCTS as the reducing and stabilizing agents, as well as a benign solvent medium, induces a good biocompatibility of AgNPs/CMCTS composite and has a wide application in biomedicine and bioanalytical fields.

Materials and methods

CMCTS (degree of substitution: 91%; degree of deacetylation: 84.0%; M_w: 3.1×10^4 Da) (Zhai et al.

2004c) was purchased from the Koyou Chemical Industrial Co. Ltd. Japan, which is in the form of sodium salt and used without further purification. CMCTS with a low molecular weight (LM-CMCTS, $M\eta = 800$ Da) was synthesized by the γ-ray irradiation of initial sample in an aqueous solution as described in our previous paper (Huang et al. 2007), then the LM-CMCTS was obtained by lyophilization. $AgNO_3$ was analytical grade and purchased from Beijing chemical plants. $HClO_4$ and NaOH were purchased from Beijing Reagent Company. All solutions were made by deionized water.

CMCTS was firstly dissolved with the deionized water. The CMCTS solution was stirred overnight and became a homogeneous system. The pH of CMCTS aqueous solution was adjusted by the 0.1 M $HClO_4$ or 0.1 M NaOH solution. After the CMCTS solution was mixed with appropriate concentration $AgNO_3$ solution, the mixture solution was bubbled with high purity N_2 for 30 min to remove oxygen and irradiated with UV light. The photochemical reactor was described in detail in a previous paper (Zhai et al. 2004a), in which the sample could be irradiated uniformly. The power and energy intensity of the middle-pressure mercury lamp are 500 W and 7×10^{-3} W/cm^2, respectively.

The UV–vis absorption spectra of AgNPs in the CMCTS solutions were obtained by a Hitachi Model 3010 spectrophotometer. The scanning wave range was from 200 to 700 nm with an interval of 0.5 nm.

The polarizing optical microscopy (POM) with a digital camera (DMLP, Leica) was used for the morphology observation of AgNPs/CMCTS composites. The optical micrograph presented in this paper was taken under a polarized light at room temperature. The samples for the POM observation were prepared by a slow evaporation method: a certain volume of AgNPs/CMCTS composite solution was added and evaporated on the surface of clean glass at the room temperature and a relative humidity of 30%.

The morphology of AgNPs in the prepared composites were also observed under a Hitachi-9000 high resolution transmission electron microscopy (HRTEM) operating at 300 kV, and the sample for inspection by the HRTEM was prepared by the slow evaporation of one drop of the dilute aqueous solution containing AgNPs/CMCTS composite on the grid of copper mesh.

The X-ray diffraction (XRD) measurement of AgNPs/CMCTS composite was carried out using a powder diffractometer (Rigaku MultiFlex) with CuKa as an X-ray source at 40 kV, 100 mA. The scattering angle (2θ) was in the range of 10–80°.

In order to study the initial process on the reduction mechanism of Ag^+ in the CMCTS solution, a laser photolysis technique was used to determine the transient absorption spectra of $AgNO_3$/CMCTS aqueous solutions in different conditions after irradiated by the pulse laser and calculate the rate constant of corresponding reduction reaction between Ag^+ and e^-_{aq}. The laser photolysis experiment was carried out in the nuclear analysis laboratory of shanghai institute of applied physics. The equipment for the laser flash photolysis experiment was described by Fu et al (Fu et al. 2006). A 266 nm (NL303HT, EKSPLA Co. in Lithuanian) excimer laser was used with the maximum energy 60 mJ of per 6 ns pulse. The analyzing light was perpendicular with the laser beam, and the optical length was 10 mm. The solution was saturated with N_2 before irradiation by pulse laser.

Results and discussion

Some polysaccharides, such as starch, cellulose derivatives and chitosan, have been used as the stabilizing agents to prepare metal nanoparticles. It is well known that polysaccharides contain nanosized inter- and intramolecular pools which can be utilized as the templates in the synthesis of nanoparticles (Raveendran et al. 2003). Furthermore, their oxygen-rich structures in the hydroxyl and ether groups lead to bind tightly with metal clusters and nanoparticles via electrostatic interactions (Huang et al. 2004). As a carboxymethylated derivative of chitosan, CMCTS has carboxyl groups in the molecular structure which can bind with metal clusters and nanoparticles stably. Recent study on the laser photolysis of CMCTS solutions revealed that there is a band at 720 nm in the transient absorption spectra, which was assigned to e^-_{aq}. It is identified that e^-_{aq} is produced from the $-NHCOCH_3$ groups of CMCTS under the irradiation of laser beam (Zhai et al. 2004c). The main reactions are illustrated as follow reactions (1)–(3), and the e^-_{aq} produced in the reaction (2) is a reducing agent for some metal cations such as Ag^+ and Au^{3+}. Thus

CMCTS can be used as both the stabilizing agent and reducing agent to synthesize metal nanoparticles by the UV light irradiation.

$$\mathrm{CMCTS} \xrightarrow{h\nu} (\mathrm{CMCTS})^{*} \quad (1)$$

$$(\mathrm{CMCTS})^{*} \rightarrow \mathrm{CMCTS}^{+} + \mathrm{e}^{-}_{\mathrm{aq}} \quad (2)$$

$$\mathrm{CMCTS} + \mathrm{e}^{-}_{\mathrm{aq}} \rightarrow \cdot\mathrm{CMCTS}^{-} \quad (3)$$

The photographs and UV–vis absorption spectra of $AgNO_3$/CMCTS mixture solutions (0.5% CMCTS and 0.5×10^{-3} mol/L $AgNO_3$) after irradiated with UV light in different pH conditions were shown in the Figs. 1 and 2a, respectively. The solutions with corresponding pH labeled on the cap of bottles were arrayed as shown in Fig. 1. The solution at pH 0.7 was almost transparent, and the solution at pH 9.6 was buff. The color of the solutions at pH 2.2 and 12.4 were yellow and dark yellow, respectively. The color change of these solutions revealed that both the amount and size of synthesized AgNPs were different in the various pH conditions.

As known from the Mie relationship (Eq. 4) (Quaranta et al. 2006) for the absorption coefficient γ of small clusters, the size and amount of nanoparticle affects both the bandwidth and the intensity of the plasmon absorption band.

$$\gamma = 18\pi \frac{N}{V} \frac{n^3}{\lambda} V_0 \frac{\varepsilon_2(\lambda)}{[\varepsilon_1(\lambda) + 2n^2]^2 + [\varepsilon_2(\lambda)]^2} \quad (4)$$

where N/V is the number of clusters per volume unit, λ is the radiation wavelength, V_0 is the cluster volume, $\varepsilon_1(\lambda)$ and $\varepsilon_2(\lambda)$ are real and imaginary parts of the silver dielectric function, which depends on both the radiation wavelength and the nanocluster size. Furthermore, dielectric materials containing nanoclusters present optical absorption bands, named surface plasmon absorption bands (SPB), which depend on both the characteristics of nanoparticles and the refractive index of the surrounding medium. However, the effect of refractive index could be omitted in our system because the pattern and intensity of SPB do not change in the solutions with the same concentrations of solutes whether we adjusted the pH of prepared AgNPs/CMCTS solutions to acidic or alkalic. It is reported that the surface plasmon excitation of AgNPs have an intense absorption peak around 400 nm. (Huang et al. 1996). As shown in Fig. 2a, the absorption peaks approximate at 410 nm (pH 2.2 and 12.4) attributed to the surface plasmon absorption of AgNPs were generally observed, and the intensity of the SPB for AgNPs was strongest in the alkalic condition

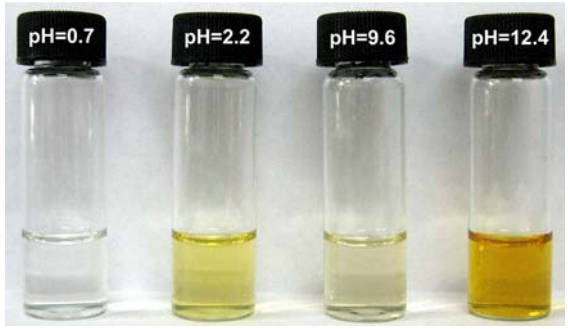

Fig. 1 Photographs of AgNPs prepared in 0.5% CMCTS and 0.5 mM $AgNO_3$ solutions with various pH

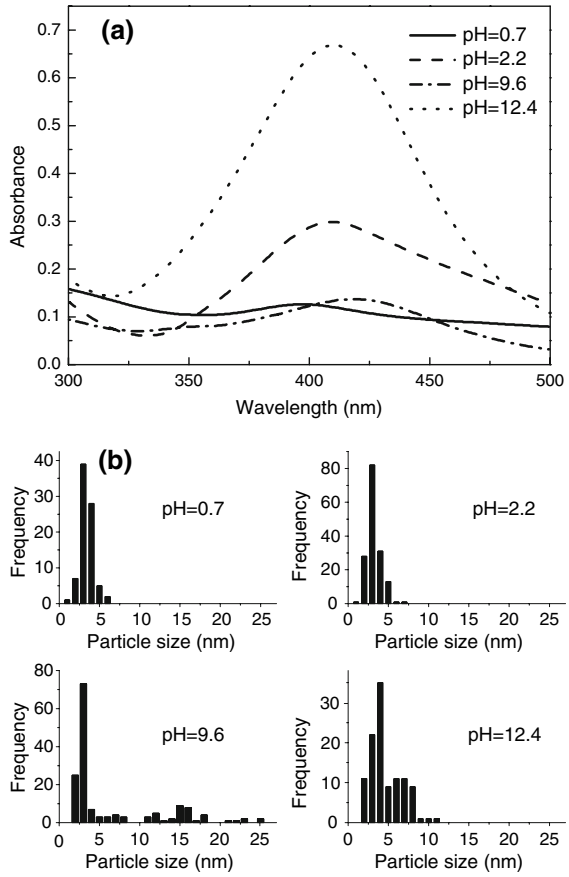

Fig. 2 (**a**) UV–vis absorption spectra of AgNPs prepared in 0.5% CMCTS and 0.5 mM $AgNO_3$ solutions with various pH; (**b**) Histograms of AgNPs size distributions in different pH conditions

(pH 12.4), which is concordant with the photograph shown in Fig. 1. Furthermore, red shift of the peak and the decrease of SPB intensity at pH 9.6 was also clearly demonstrated in Fig. 2a. Heard et al. (Heard et al. 1983) found that SPB of AgNPs shifts toward longer wavelengths as the size of AgNPs is increased. With the aid of HRTEM photographs, the size statistics of AgNPs formed in various pH solutions were showed in Fig. 2b. The peak in pH 0.7 condition was weak and has a short maximum absorption wavelengths, it is because both the amount and size of AgNPs are small in this condition. The size and amount of AgNPs are increased to a certain extent when the pH of solution increased to 2.2. As the pH reached 9.6, the size of AgNPs increased remarkably and the size distribution became wide. That is the reason that the corresponding absorption peak in Fig. 2a became wide and has certain red shift. Thus we can speculate that AgNPs formed at pH 9.6 solutions were different from those at other pH conditions. Furthermore, the size of AgNPs mainly distributed in 2–8 nm in the pH 12.4 conditions, thus relative large size and narrow size distribution led to the strongest SPB as showed in Fig. 2a. The effect of pH on the size and amount of AgNPs synthesized in the present method is complicated. On the one hand, pH has a direct influence on the reactive mode of the reducing agent (e^-_{aq}). For example, the SPB at pH 0.7 was very weak owing to the rapid decay of e^-_{aq} in the strong acidic condition (reaction (5)). At the same time, the intensity of SPB for AgNPs was weaker at pH 2.2 than that at pH 12.4 due to the same reason too.

$$e^-_{aq} + H^+ \rightarrow \cdot H \quad (5)$$

On the other hand, there is a pH dependence of the conformation of macromolecules in the CMCTS aqueous solutions (Zhai et al. 2004b). When the pH of CMCTS solution was in a range of 4.0–7.3, uncharged CMCTS chains shrink to a coiled state, leading to a decrease of the concentration of AgNPs. In the case of lower pH (<4.0) or higher pH (>7.3), the electrostatic repulsion effect among the protonated amino groups ($-NH_3^+$) or unprotonated carboxyl groups ($-COO^-$) will make the chains in the dissociated state stretch and form a rodlike conformation. Such a linear conformation of polysaccharides can fabricate nanosize templates conveniently for the synthesis of AgNPs. In the pH 9.6 solutions, the coiled conformation of CMCTS resulted in the large size and wide distribution of AgNPs when the pH of solution was closed to the isoelectric point of CMCTS. Furthermore, the effect of pH on the stability of AgNPs was also monitored by observing the occurrence of precipitation. These AgNPs were suspended steadily in the alkalic CMCTS solutions (pH = 12.4) at least for 6 months. However, black precipitation can be observed in the acidic solution (pH 0.7 and pH 2.2) within 24 h, indicating that pH 12.4 is an ideal condition for synthesizing and preserving AgNPs in the CMCTS solutions. We speculated that the change of carboxyl groups of CMCTS with pH played an important role in the formation of stable AgNPs. At pH 12.4, the electrostatic attractive interaction between charged AgNPs and the $-COO^-$ of CMCTS chain lead to the stabilization of AgNPs; but at pH 2.2, the $-COO^-$ of CMCTS change into –COOH, which formed strong hydrogen bonds with each other (Mayya et al. 1997) and led to the aggregation and precipitation of AgNPs. Thus in the following experiment, pH 12.4 was selected as the optimal pH condition for synthesizing AgNPs.

The influences of the concentrations of CMCTS and $AgNO_3$ on the SPB of AgNPs are shown in Fig. 3a and b, respectively. When the concentration of CMCTS was decreased from 0.5 to 0.1%, the intensity of SPB decreased to the minimum and a tiny red shift of SPB occurred, and the intensity of SPB increased with a further decrease of the concentration of CMCTS from 0.1 to 0.033%. Simultaneously, a blue shift of SPB can be observed. Thus it revealed that the change of concentrations of CMCTS altered the number of nucleation presented by CMCTS and the size of AgNPs. As identified by Esumi et al. (Esumi et al. 2003), who have presented detailed illumination by TEM photograph about the size of gold nanoparticles increased to a maximum then decreased with an increase of the chitosan concentration. Based on their conclusion, we speculated that interaction sites with various pools as nucleation templates can be formed in the alkalic CMCTS solutions with different concentrations. When the concentration of CMCTS is high (0.1–0.5%), the nucleation templates are mostly formed by the coiling of CMCTS macromolecular chains and limit the activity of CMCTS and Ag^+. With the decrease of CMCTS concentration, some large templates will be formed and result in the decreasing amount of AgNPs

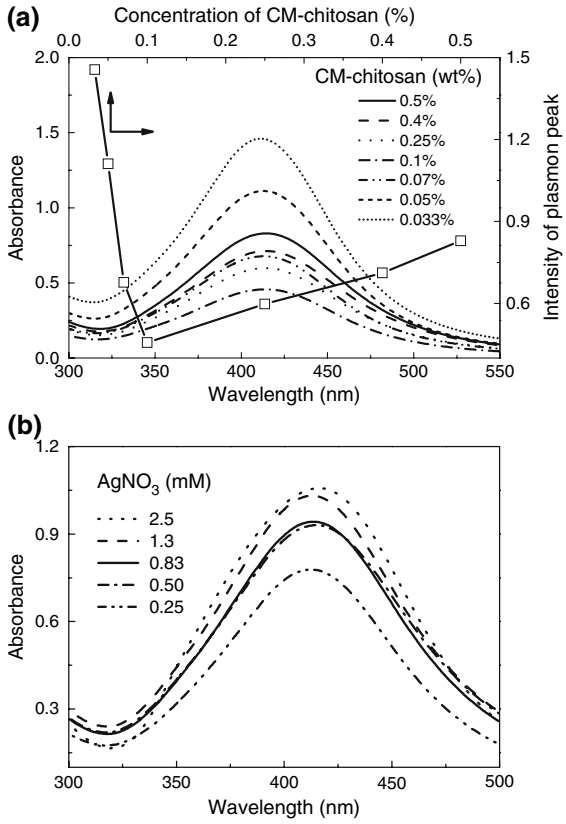

Fig. 3 UV–vis absorption spectra of AgNPs prepared with (**a**) 0.5 mM $AgNO_3$ and various concentrations of CMCTS, pH 12.4, (**b**) 0.5% CMCTS and various concentrations of $AgNO_3$, pH 12.4

but an increasing size of AgNPs, which induced the decrease in the SPB at 410 nm. Some CMCTS macromolecular chains begin to be free from the coiled state until the concentration of CMCTS reached a critical value (0.1%). Below this concentration (<0.1%), small sized AgNPs can be produced with the aid of thermal movement of CMCTS and Ag^+. Thus the decrease of CMCTS concentration resulted in a decrease of AgNPs size, but an increase of nucleation amount (Huang et al. 2004). That was the reason why the SPB at 410 nm was increased with a further decrease concentration of CMCTS from 0.1 to 0.033%.

As shown in Fig. 3b, with the increase of $AgNO_3$ concentration from 0.25 to 2.5 mM, the intensity of SPB increased and the band has some red shift. Furthermore, the obvious color change of these solutions from buff to dark yellow with an increase of Ag^+ concentration can be observed, too. Heard et al. (1983) and Long et al. (2007) have found that the SPB shifts toward longer wavelength as the size of particle increases as mentioned in the previous section. Thus it is apparent that the size of AgNPs was increased with the increase of Ag^+ concentration, and the amount of small sized AgNPs was increased because the number of nucleation was increased.

Not only a bactonet-like structure for the composite of AgNPs and chitosan, but also the branch-like structure for the composites of some noble metal particles (Au, Pt and Pd) and chitosan can be observed in the POM images (Huang et al. 2004). How about the morphology of AgNPs/CMCTS composite? A branch-like structure can also be clear observed in the POM image, as it was shown in Fig. 4. The amplification factor was 400 and the branch-like samples prepared with 0.02% CMCTS and 0.24 mM $AgNO_3$ (pH 12.4) were observed with a polarized light. It was identified that an alkalic CMCTS solution without $AgNO_3$ added can also form such a branch-like structure. Figure 5a and b, which showed that AgNPs were synthesized with 0.25% CMCTS and 1.2 mM $AgNO_3$ (pH 12.4) within or on the surface of CMCTS matrix homogeneously, are TEM images of AgNPs/CMCTS composites with the amplification factors of 10^4 and 2×10^5, respectively. In Fig. 5a, a fined branch-like structure can also be observed clearly as shown in Fig. 4, but AgNPs can not be observed immediately.

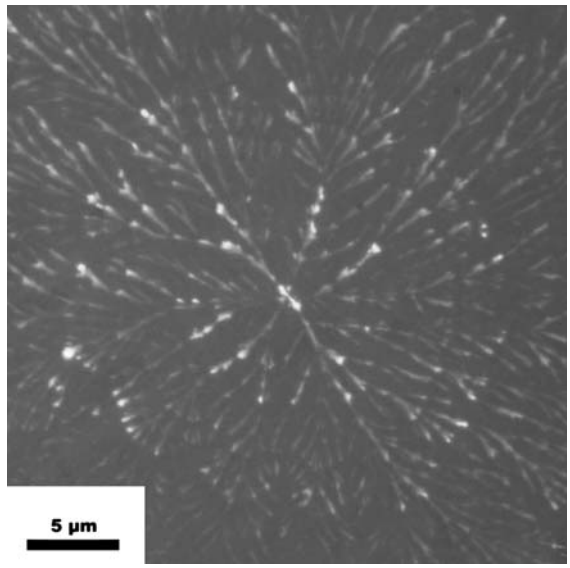

Fig. 4 POM graphs of AgNPs/CMCTS composites prepared with 0.02% CMCTS and 0.24 mM $AgNO_3$, pH 12.4

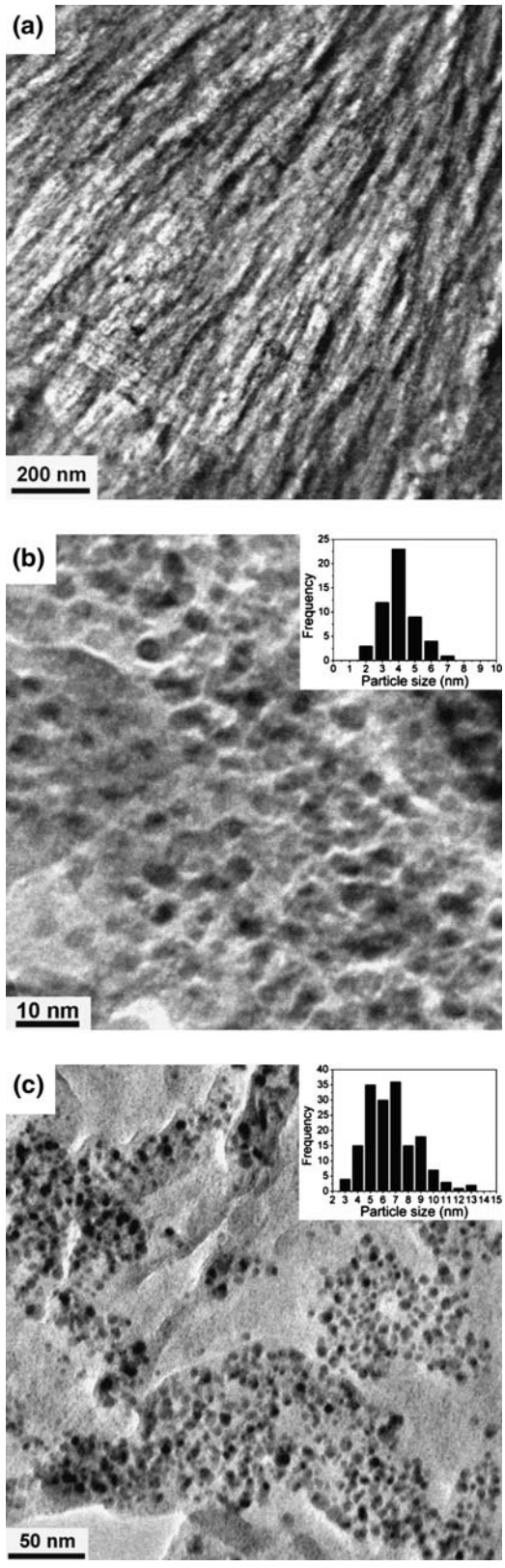

Fig. 5 TEM images of AgNPs/CMCTS composites prepared with 0.25% CMCTS and 1.2 mM $AgNO_3$, pH 12.4. (**a**) $M\eta$ of CMCTS was 30000 Da, amplification factor: 10^4 (**b**) $M\eta$ of CMCTS was 30000 Da, amplification factor: 2×10^5 (**c**) $M\eta$ of CMCTS was 800 Da, amplification factor: 5.3×10^4, and histograms of particle size distributions (inset)

When we turned the amplification factor up to 2×10^5, the AgNPs possessing a diameter range of 2–8 nm were presented within and on the surface of CMCTS matrices, and the size distribution was very narrow. It is reported that the size of AgNPs synthesized by heparin reduction (Huang and Yang 2004b) was in the range of 9–29 nm, and the size of AgNPs synthesized by the electron irradiation (Bogle et al. 2006) was in the range of 10–60 nm. The size of AgNPs obtained in our method was much smaller and more even than that of these previous reported methods. Furthermore, LM-CMCTS replaced CMCTS for the synthesis of AgNPs in the same condition, and the TEM image of AgNPs/LM-CMCTS composites in Fig. 5c showed a different pattern in Fig. 5b. However, no branch-like structure was formed. Replaced by a homogeneous thin film can be observed, on which AgNPs with a diameter range of 3–13 nm were distributed unevenly. Contrasted with Fig. 5b and c, we can notice that the diameter of AgNPs synthesized in the LM-CMCTS solution was larger than that of AgNPs synthesized in the CMCTS solution. What is more, the size distribution of AgNPs synthesized in the LM-CMCTS solution was wider than that of AgNPs synthesized in the CMCTS solution. It could be explained that without any size-confined influence for the movement of LM-CMCTS chains resulted to the increase of nucleation and a low size-confined influence on the growth of AgNPs. On the other side, because LM-CMCTS can not form stable templates for the synthesis of AgNPs, LM-CMCTS was not an ideal stabilizing agent for AgNPs despite AgNPs were proved to be synthesized more easily and quickly in its solutions. It was identified that AgNPs formed in LM-CMCTS solution were found to precipitate within 1 month. Thus LM-CM-chitoan was not adoptable to synthesize and stabilize the metal nanoparticles as much as CMCTS was.

The formation of AgNPs in a 0.25% CMCTS and 1.2 mM $AgNO_3$ solution (pH 12.4) was confirmed by using the XRD pattern. Figure 6 showed the diffraction peaks for CMCTS stabilized AgNPs, which were

obtained after drying at 60 °C for 24 h. Except for the peaks belonging to CMCTS, we can see four strong Bragg diffraction peaks at 38.1°, 44.3°, 64.4° and 77.5° which pertain to 111, 200, 220, 311 planes of a face centered cubic (fcc) lattice of silver, respectively (Bogle et al. 2006). The value of lattice constant obtained from the XRD pattern was found to be consistent with that given by PDF No. 4-0783 as well. The XRD pattern revealed that AgNPs synthesized in the present method were in the conformation of cubic crystal structure.

It is reported that the Ag° formed in the initial reducing reaction (6) has an absorption band at 360 nm and the molar absorbance coefficient of Ag° is $1.6 \times 10^4\ M^{-1}\ cm^{-1}$ (Ershov et al. 1993b), then the band shifts to 310 and 265 nm due to the formation of Ag_2^+ after the coalescence processes between Ag° and Ag^+ (reaction (7)) (Ershov et al. 1993a). After Ag_2^+ is coalesced with more Ag^+ ions by reaction (8), oligomeric clusters appear step by step and form stable complexes with CMCTS due to the high affinity between Ag clusters and CMCTS. When these complexes are further reduced, larger cluster and finally AgNPs are present (Ershov and Henglein 1998).

$$Ag^+ + e_{aq}^- \xrightarrow{k_1} Ag^\circ \quad k_1 = 3 \times 10^{10}\ M^{-1}\ s^{-1} \tag{6}$$

$$Ag^\circ + Ag^+ \xrightarrow{k_2} Ag_2^+ \quad k_2 = 5 \times 10^9\ M^{-1}\ s^{-1} \tag{7}$$

$$Ag_2^+ + Ag^+ \xrightarrow{k_3} Ag_3^{2+} \rightarrow \cdots \rightarrow Ag_n^+ \quad k_3 = 2 \times 10^9\ M^{-1}\ s^{-1} \tag{8}$$

In our previous work, it has found that photolysis of aqueous solution of CMCTS by 248 nm excimer laser led to the formation of e_{aq}^- (Zhai et al. 2004c). The signal of e_{aq}^- can also be observed when the solution of CMCTS was radiated by 266 nm excimer laser, and the signal of e_{aq}^- decreases with adding $AgNO_3$ in the CMCTS solution, as it was shown in Fig. 7. In order to investigate the reaction between Ag^+ ions and e_{aq}^-, the solutions containing 0.25% CMCTS and $AgNO_3$ with different concentrations (0.13–2.5 mM) was irradiated by a 266 nm excimer laser, and the absorption decay of e_{aq}^- at 720 nm was monitored simultaneously. The rate constant (k) between e_{aq}^- and Ag^+ ions was calculated from the dependence of observed pseudo-first-order decay (k_{obsd}) on the concentration of Ag^+ using the Eq. 9.

$$k_{obsd} = A + k[Ag^+] \tag{9}$$

The rate constant of the reaction between e_{aq}^- and Ag^+ obtained from the slope of fitted line in Fig. 8 was $5.0 \times 10^9\ M^{-1}\ s^{-1}$. A good linear relationship ($r = 0.99$) between k_{obsd} and the concentration of Ag^+ was obtained too. The high rate constant shows that Ag^+ ions can be reduced conveniently to Ag° in the CMCTS solutions by the UV light irradiation, but the value is smaller than the quoted value of $3 \times 10^{10}\ M^{-1}\ s^{-1}$ (Ershov and Henglein 1998), which was obtained for the reaction in the absence of CMCTS. It is because the interaction between CMCTS and Ag^+ might inhibit the reductive reaction (6). In addition, e_{aq}^- also react with CMCTS (reaction (3)), although its rate constant was less than 0.1% of that of the

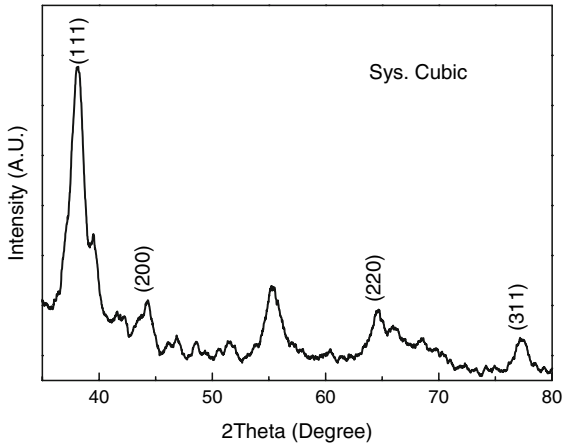

Fig. 6 XRD pattern of UV-induced AgNPs/CMCTS composites prepared with 0.25% CMCTS and 1.2 mM $AgNO_3$, pH 12.4

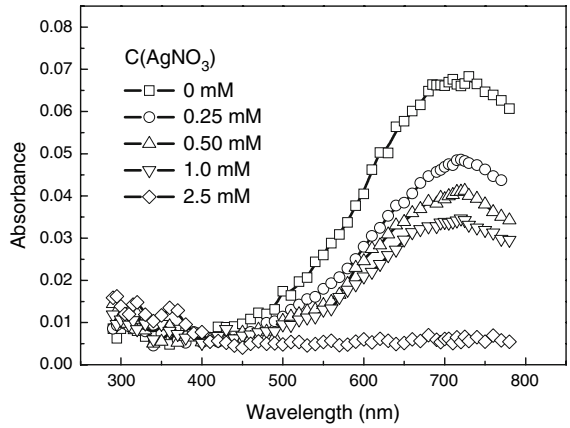

Fig. 7 Transient absorption spectra (0.1 μs) observed on laser photolysis of 0.25% CMCTS and various concentrated $AgNO_3$ solutions saturated with N_2, pH 9.5

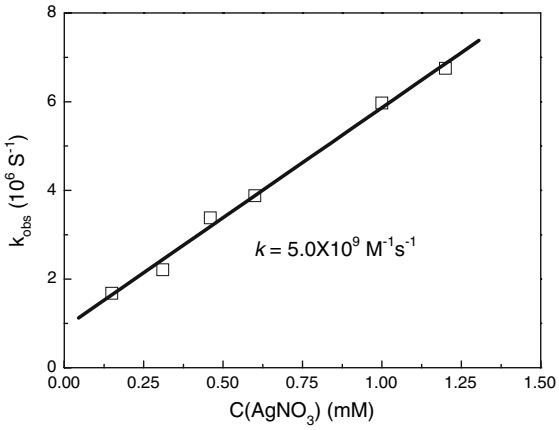

Fig. 8 Dependence of pseudo-first-order decay rate constant of e^-_{aq} on $AgNO_3$ concentration in 0.25% CMCTS solution, pH 9.5

reaction between e^-_{aq} and Ag^+ ions (Cheng et al. 2005). As it is shown in Fig. 9, the band appeared at 370 nm and observable within 15 μs after the solution containing 0.25% CM-chitsoan and 2.5 mM $AgNO_3$ were irradiated by the pulse laser. Furthermore, the intensity of this band was increased with the increase of concentration of Ag^+ as Fig. 7 was shown, and this band can not be observed in the neat CMCTS solution irradiated by the pulse laser. Thus we assign this band to the absorption of Ag°. The decay of the band was occurred because Ag° can react with Ag^+ to form an oligomeric cluster by reaction (7). Comparing with the result reported by

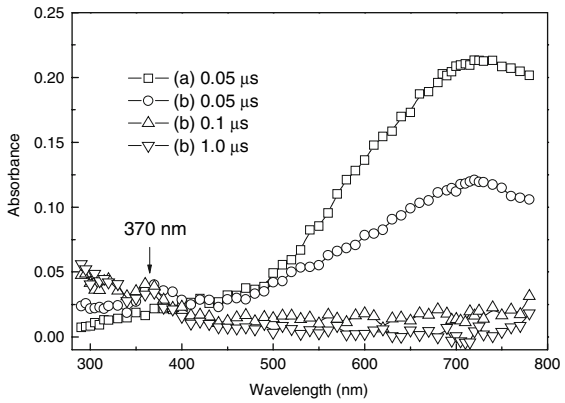

Fig. 9 Transient absorption spectra of N_2-satured aqueous solutions containing (**a**) 0.25% CMCTS, pH 9.5; (**b**) 0.25% CMCTS and 2.5 mM $AgNO_3$ obtained by 266 nm laser photolysis, pH 9.5

Ershov et al. (Ershov et al. 1993b), CMCTS also has effect on the intensity of absorption band of Ag°.

$$Ag_n^+ + \cdot CMCTS^- \xrightarrow{H_2O} Ag_n \cdots CMCTS \qquad (10)$$

The growth of AgNPs by the reduction of Ag^+ to Ag_n^+ in CMCTS solutions is stepwise as mentioned in the reactions (6)–(8). Finally, a biocompatible AgNPs/CMCTS composite were formed through reaction (10).

Conclusion

The biocompatible AgNPs were synthesized in a green and convenient method in the alkalic $AgNO_3$/CMCTS aqueous solution by the UV light irradiation. The UV–vis absorption spectra and TEM images revealed that both the concentrations of $AgNO_3$ and CMCTS, which acted as a reducing agent and a stabilizing agent, have effect on the size and amount of AgNPs. The morphology of AgNPs/CMCTS composites was branch-like under POM and TEM observation. Cubic crystal AgNPs prepared in this new method can be dispersed stably in the alkaline CMCTS solution for more than 6 months. The Spectra of laser photolysis of $AgNO_3$/CMCTS aqueous solution revealed that Ag^+ were reduced by e^-_{aq}, and the rate constant of reduction reaction was 5.0×10^9 M^{-1} s^{-1} in the 0.25% CMCTS aqueous solution. Owing to the good biocompatibility of CMCTS, the AgNPs synthesized in the present work have potential applications in biological medicine field.

Acknowledgments The National Natural Science Foundation of China (NNSFC, Project No. 50473017) and The Key Project of Ministry of Education of China (Project No.105003) are acknowledged for supporting this research.

References

Belloni J (1996) Metal nanocolloids. Curr Opin Colloid Interface Sci 1:184–196

Bogle KA, Dhole SD, Bhoraskar VN (2006) Silver nanoparticles: synthesis and size control by electron irradiation. Nanotechnology 17:3204–3208

Cao JM, Zheng MB, Lu P, Deng SG, Chen YP, Wen F, Guo J, Zhang F, Tao J (2005) Sythesis of silver nanoparticles by reductive polysaccharides. Acta Chim Sin 63:1541–1544

Chen Q, Liu SQ, Du YM, Peng H, Sun LP (2006) Carboxymethyl-chitosan protects rabbit chondrocytes from interleukin-1 beta-induced apoptosis. Eur J Pharmacol 541:1–8

Cheng DM, Zhou XD, Xia HB, Chan HSO (2005) Novel method for the preparation of polymeric hollow nanospheres containing silver cores with different sizes. Chem Mater 17:3578–3581

Ershov BG, Henglein A (1998) Time-resolved investigation of early processes in the reduction of Ag^+ on polyacrylate in aqueous solution. J Phys Chem B 102:10667–10671

Ershov BG, Janata E, Henglein A (1993a) Growth of silver particles in aqueous solution: long-lived "magic" clusters and ionic strength effects. J Phys Chem 97:339–343

Ershov BG, Janata E, Henglein A, Fojtik A (1993b) Silver atoms and clusters in aqueous solution: absorption spectra and the particle growth in the absence of stabilizing Ag^+ ions. J Phys Chem 97:4589–4594

Esumi K, Takei N, Yoshimura T (2003) Antioxidant-potentiality of gold-chitosan nanocomposites. Colloid Surf B 32:117–123

Fang Q, He G, Cai WP, Zhang JY, Boyd IW (2004) Palladium nanoparticles on silicon by photo-reduction using 172 nm excimer UV lamps. Appl Surf Sci 226:7–11

Fu HY, Wu GZ, Long DW, Liu YD, Wang WF, Yao SD (2006) Studies of $[Me_3NC_2H_4OH]Zn_2Cl_5$ aqueous solution by laser photolysis. Acta Chim Sin 64:483–488

Hayward RC, Saville DA, Aksay IA (2000) Electrophoretic assembly of colloidal crystals with optically tunable micropatterns. Nature 404:56–59

Heard SM, Grieser F, Barraclough CG, Sanders JV (1983) The characterization of silver sols by electron microscopy, optical absorption, and electrophoresis. J Colloid Interface Sci 93:545–555

Henglein A (1998) Colloidal silver nanoparticles: Photochemical preparation and interaction with O_2, CCl_4, and some metal ions. Chem Mater 10:444–450

Huang HZ, Yang XR (2004a) Synthesis of chitosan-stabilized gold nanoparticles in the absence/presence of tripolyphosphate. Biomacromolecules 5:2340–2346

Huang HZ, Yang XR (2004b) Synthesis of polysaccharide-stabilized gold and silver nanoparticles: a green method. Carbohydr Res 339:2627–2631

Huang HH, Ni XP, Loy GL, Chew CH, Tan KL, Loh FC, Deng JF, Xu GQ (1996) Photochemical formation of silver nanoparticles in poly(N-vinylpyrrolidone). Langmuir 12:909–912

Huang HZ, Yuan Q, Yang XR (2004) Preparation and characterization of metal-chitosan nanocomposites. Colloid Surf B 39: 31–37

Huang HZ, Qiang Y, Yang XR (2005) Morphology study of gold-chitosan nanocomposites. J Colloid Interface Sci 282:26–31

Huang L, Zhai ML, Peng J, Li JQ, Wei GS (2007) Radiation-induced degradation of carboxymethylated chitosan in aqueous solution. Carbohydr Polym 67:305–312

Long DW, Wu GZ, Chen SM (2007) Preparation of oligochitosan stabilized silver nanoparticles by gamma irradiation. Radiat Phys Chem 76:1126–1131

Mayya KS, Patil V, Sastry M (1997) On the stability of carboxylic acid derivatized gold colloidal particles: the role of colloidal solution pH studied by optical absorption spectroscopy. Langmuir 13:3944–3947

Pastoriza-Santos I, Liz-Marzan LM (2002) Formation of PVP-protected metal nanoparticles in DMF. Langmuir 18:2888–2894

Quaranta A, Carturan S, Bonafini M, Maggioni G, Tonezzer M, Mattei G, de Julian Fernandez C, Della Mea G, Mazzoldi P (2006) Optical sensing to organic vapors of fluorinated polyimide nanocomposites containing silver nanoclusters. Sens Actuators B Chem 118:418–424

Raveendran P, Fu J, Wallen SL (2003) Completely "green" synthesis and stabilization of metal nanoparticles. J Am Chem Soc 125:13940–13941

Sakai H, Kanda T, Shibata H, Ohkubo T, Abe M (2006) Preparation of highly dispersed core/shell-type titania nanocapsules containing a single Ag nanoparticle. J Am Chem Soc 128:4944–4945

Son WK, Youk JH, Park WH (2006) Antimicrobial cellulose acetate nanofibers containing silver nanoparticles. Carbohydr Polym 65:430–434

Sudeep PK, Kamat PV (2005) Photosensitized growth of silver nanoparticles under visible light irradiation: a mechanistic investigation. Chem Mater 17:5404–5410

Van Hyning DL, Klemperer WG, Zukoski CF (2001) Silver nanoparticle formation: Predictions and verification of the aggregative growth model. Langmuir 17:3128–3135

Zhai ML, Chen YF, Yi M, Ha HF (2004a) Swelling behaviour of a new kind of polyampholyte hydrogel composed of dimethylaminoethyl methacrylate and acrylic acid. Polym Int 53:33–36

Zhai ML, Kudoh H, Wach RA, Wu GZ, Lin MZ, Muroya Y, Katsumura Y, Zhao L, Nagasawa N, Yoshii F (2004b) Laser photolysis of carboxymethylated chitin derivatives in aqueous solution. Part 2. Reaction of ·OH and $\cdot SO_4^-$ radicals with carboxymethylated chitin derivatives. Biomacromolecules 5:458–462

Zhai ML, Kudoh H, Wu GZ, Wach RA, Muroya Y, Katsumura Y, Nagasawa N, Zhao L, Yoshii F (2004c) Laser photolysis of carboxymethylated chitin derivatives in aqueous solution. Part 1. Formation of hydrated electron and a long-lived radical. Biomacromolecules 5:453–457